Published in final edited form as:
Biochim Biophys Acta. 2011 March ; 1811(3): 163–169. doi:10.1016/j.bbalip.2010.12.006.

Valproate uncompetitively inhibits arachidonic acid acylation by rat acyl-CoA synthetase 4: Relevance to valproate's efficacy against bipolar disorder

Jakob A. Shimshoni[1,2,+], **Mireille Basselin**[1], **Lei O. Li**[3], **Rosalind A. Coleman**[3], **Stanley I. Rapoport**[1], and **Hiren R. Modi**[1,*,+]

[1] Brain Physiology and Metabolism Section, National Institute on Aging, National Institutes of Health, Bethesda, MD, USA

[3] Department of Nutrition, University of North Carolina, Chapel Hill, NC, USA

Abstract

Background—The ability of chronic valproate (VPA) to reduce arachidonic acid (AA) turnover in brain phospholipids of unanesthetized rats has been ascribed to its inhibition of acyl-CoA synthetase (Acsl)-mediated activation of AA to AA-CoA. Our aim was to identify a rat Acsl isoenzyme that could be inhibited by VPA *in vitro*.

Methods—Rat Acsl3-, Acsl6v1- and Acsl6v2-, and Acsl4-flag proteins were expressed in *E. coli*, and the ability of VPA to inhibit their activation of long-chain fatty acids to acyl-CoA was estimated using Michaelis-Menten kinetics.

Results—VPA uncompetitively inhibited Acsl4-mediated conversion of AA and of docosahexaenoic (DHA) but not of palmitic acid to acyl-CoA, but did not affect AA conversion by Acsl3, Acsl6v1 or Acsl6v2. Acsl4-mediated conversion of AA to AA-CoA showed substrate inhibition and had a 10-times higher catalytic efficiency than did conversion of DHA to DHA-CoA. Butyrate, octanoate, or lithium did not inhibit AA activation by Acsl4.

Conclusions—VPA's ability to inhibit Acsl4 activation of AA and of DHA to their respective acyl-CoAs, related to the higher catalytic efficiency of AA than DHA conversion, may account for VPA's selective reduction of AA turnover in rat brain phospholipids, and contribute to VPA's efficacy against bipolar disorder.

Keywords

bipolar disorder; valproate; arachidonic acid; acyl-CoA synthetase; mood stabilizer; Acsl4; brain; rat

[*]Corresponding author: Hiren R. Modi, Ph.D. Brain Physiology and Metabolism Section, National Institute on Aging, National Institutes of Health, Bldg. 9, Rm. 1S126; 9000 Rockville Pike, Bethesda, MD 20892. modihr@mail.nih.gov, Tel: 301 594 5076; Fax: 301 402 0074.
[2]Present address: Department of Pharmaceutics, University of Washington, Seattle, WA, USA
[+]Each author contributed equally to this paper

Disclosure/Conflict of interest.
No author has a financial or other conflict of interest related to this work.

INTRODUCTION

Valproate (VPA), a branched-chain achiral eight-carbon isooctanoic acid, is approved by the FDA for treating bipolar disorder (BD), but it is teratogenic and its efficacy against BD is incomplete [1]. Understanding the mechanism of action of VPA and its brain target as a basis of its efficacy against BD may help to design more effective, less toxic drugs [2].

One suggested mechanism of action of VPA against BD, as well as of carbamazepine and lithium, is based on evidence that each of these mood stabilizers, when given chronically to rats to produce therapeutically relevant plasma concentrations, downregulated arachidonic acid (AA, 20:4n-6) but not docosahexaenoic acid (DHA, 22:6n-3) or (in the case of lithium) palmitate (16:0) turnover in brain phospholipids. This common effect agrees with the fact that the postmortem BD brain demonstrates upregulated markers of AA metabolism, associated with neuroinflammation, excitotoxicity and apoptosis [2–5]. Similar associations between these neuropathological processes and upregulated brain AA metabolic markers have been identified in animal models [6–8].

Reduced brain AA turnover in unanesthetized rats given lithium or carbamazepine correlates with downregulation of mRNA, protein and activity of Ca^{2+}-dependent cytosolic phospholipase A_2 ($cPLA_2$) type IV, which selectively hydrolyzes AA (compared with DHA) from membrane phospholipid *in vitro* [2,9,10], as well with reduced activity of cyclooxygenase (COX)-2; COX-2 is functionally coupled to $cPLA_2$ and converts AA to prostaglandin E_2 and other proinflammatory eicosanoids [11–14]. Chronic VPA did not downregulate rat brain $cPLA_2$, but did reduce net brain COX activity and protein levels of both COX-1 and COX-2 [15]. VPA also reduced the rate of conversion of AA to AA-CoA, but not of DHA to DHA-CoA, in a rat brain microsomal fraction having acyl-CoA synthetase (Acsl, E.C.6.2.1.3) activity [16]. VPA itself is not a substrate for rat brain microsomal Acsl [16], and neither valproyl-CoA nor esterified VPA was found in the brain of rats following chronic administration of the drug [17]. Inhibition of conversion to acyl-CoA may underlie VPA's selective reduction of AA turnover in rat brain phospholipids *in vivo* [18].

Twenty-six human ACSL genes have been identified within five subfamilies, based on chain length of the preferred acyl groups [19]. Five human long-chain Acsl proteins have been characterized, represented by multiple splice variants, yielding 15 isoenzymes that preferably acylate fatty acids of 12–22 carbon length. In rats, each of four ACSL genes (ACSL1, ACSL3, ACSL4, and ACSL5) is represented by only one variant, whereas ACSL6 is represented by two splice variants (ACSL6v1 and ACSL6v2) [20]. Each isozyme has a distinct tissue distribution, subcellular location and fatty acid preferences. Acsl3, Acsl6v1, and Acsl6v2 are the predominant isoforms in rat brain, whereas Acsl1 and Acsl5 are expressed mainly in liver and adipose tissue [21–23]. Acsl3 and Acsl 6 act on AA preferentially among C_{14}–C_{22} unsaturated fatty acids, compared to Acsl1 and Acsl5 [23]. Acsl4 has a marked preference for AA [23], and is expressed in neurons but not glial cells in the human cerebellum and hippocampus, where it may be required for dendritic spine formation [24,25]. No mammalian Acsl enzyme has been crystallized or has a published structure.

In view of the finding that conversion of AA compared with DHA to its respective acyl-CoA by the rat brain microsomal fraction was inhibited by VPA [16], we thought it worthwhile to try to identify a specific rat Acsl whose conversion of AA to AA-CoA could be inhibited by VPA. To do this, we quantified inhibition by VPA of AA, DHA and palmitic acid conversion to their respective acyl-CoAs with recombinant rat Acsl3, Acsl4 and Acsl6 isoenzymes. We did not study Acsl1 or Acsl5 because of their reported low selectivity for

AA and their low distribution in the brain compared to the other three Acsl isoenzymes (see above).

Material and methods

Reagents

[1-^{14}C]AA (50 mCi/mmol), [1-^{14}C]DHA (56 mCi/mmol) and [^{14}C]palmitic acid (56 mCi/mmol) were purchased from Moravek Biochemicals (Brea, CA). Fatty acids, sodium VPA, sodium octanoate, sodium butyrate, triacsin C, LiCl, coenzyme A, ATP, anti-Flag M2 monoclonal mouse antibody, and goat anti-mouse IgG-peroxidase conjugate were purchased from Sigma (St. Louis, MO).

Preparation of bacterial lysate

Recombinant plasmids for rat brain ACSL3, ACSL6v1 and ACSL6v2, and for rat liver ACSL4-Flag, were expressed in *E. Coli* strain BL21-codonPlus (DE3)-RIL [20,26,27]. As a negative control, the same strain, transformed with the empty vector, was used under identical conditions. Recombinant Acsl-Flag proteins were induced with 1 mM isopropyl-β-D-1-thiogalactopyranoside (IPTG) at A_{600} = 1.0. *E. Coli* was grown in Terrific Broth medium supplemented with carbenicillin (final concentration 50 μg/ml) at 37 °C and shaken at 206 rpm. After a 6-h induction, cells were harvested by centrifugation at 4000 g for 20 min in a Sorval SA-600 rotor at 4°C. The cell pellet was resuspended in a buffer containing 10 mM HEPES (pH 7.8) and 0.5 mM EDTA, and sonicated on ice with six 10-s bursts each followed by a 10-s rest, using a cell disruptor sonicator (Heat Systems Ultrasonics, Farmingdale, NY) at setting 4. Lysate aliquots were stored at −80°C for enzyme assay. Protein concentrations were determined by the Bradford method [28].

Relative Protein Determination and Western Blot Analysis

Cell lysates (1 μg) of each isozyme were separated by electrophoresis on a 10–20% SDS-PAGE, transferred to a polyvinylidene fluoride membrane (Bio-Rad), and incubated with anti-Flag M2 monoclonal antibody. For chemiluminescence detection, immunoreactive bands were visualized by incubating the membranes with horseradish peroxidase-conjugated antibodies followed by PicoWest reagents (Thermo Fisher Scientific, Rockford, IL). NIH ImageJ software was used for densitometry analysis. The amount of final cell-lysate per tube (1 μg) was normalized to the band intensity of each isozyme, yielding the relative isozyme concentration.

Acsl Activity Assay

Acsl activity was measured using 1–3 μg protein. The assay medium contained 175 mM Tris-HCl pH 7.4, 8 mM $MgCl_2$, 5 mM dithiothreitol, 10 mM ATP, 0.25 mM CoA, 0.01 mM EDTA, and 5 μM [^{14}C]fatty acid in 0.5 mM Triton X-100, and increasing concentrations of the unlabeled fatty acids in a total volume of 200 μl. Sodium VPA (0, 10, 30, 60 or 90 mM) or lithium chloride (0, 10 or 30 mM) was added directly to the reaction mixture during inhibition assays. Triacsin C, an inhibitor of Acsl1, Acsl3 and Acsl4 [27], was added directly to the reaction mixture at 10 μM as a positive control. As additional controls, sodium octanoate (a constitutional isomer of VPA) or sodium butyrate (a short-chain VPA analogue) was added to the reaction mixture at 60 mM. Assays were performed at 37°C for 5 min with shaking. The reaction was started by adding 15 μl bacterial lysate to the reaction mixture, and was terminated by adding 1 ml Dole's Reagent (isopropanol:heptane:1 M H_2SO_4, 80:20:2, by vol). In a preliminary experiment, the pH of reaction mixtures spiked with VPA and sodium octanoate at concentrations of 60 and 90 mM was measured using a pH meter. The pH (7.4) remained constant at these drug concentrations. Unesterified fatty

acids were removed with two 2-ml heptane washes and acyl-CoA radioactivity was measured by liquid scintillation counting. As a negative control, Acsl enzyme activity of the *E. Coli* cell lysate lacking a gene coding for ACSL-Flag was measured with AA as substrate as described above. The results were corrected for blanks (samples without cell lysates added and samples analyzed in the absence of fatty acids).

Analysis and Statistics

For each Acsl, initial reaction velocity V was plotted against substrate concentrations at each VPA concentration I_o and the plots were fitted by least squares to a hyperbolic Michaelis-Menten model using GraphPad Prism version 5.00 (GraphPad Software, San Diego, CA). K_m (μM) and V_{max} (nmol/min/mg protein) were calculated by the following equation, in which V is reaction velocity (nmol acyl-CoA formed/min/mg enzyme protein, e.g. nmol/min/mg protein) at a given fatty acid substrate concentration, S (μM),

$$V=\frac{V_{\max}S}{K_m+S} \quad (1)$$

Catalytic efficiency, which reflects turnover of the enzyme, was calculated from the ratio of V_{max} to K_m, normalized to the relative enzyme concentration (E_T, mg/l) [29],

$$\text{Catalytic Efficiency}=\frac{V_{\max}}{K_m E_T} \quad (2)$$

The model in which substrate inhibits reaction velocity can be described as [30],

$$V=\frac{V_{\max}S}{K_m+S\left(1+\frac{S}{K_s}\right)} \quad (3)$$

A model that involves both substrate inhibition and uncompetitive inhibition by inhibitor I_o can be represented as,

$$V=\frac{V_{\max}S}{K_m+S\left(1+\frac{S}{K_S}+\frac{I_o}{K_i}\right)} \quad (4)$$

where K_i is the enzyme inhibition constant.

Data were plotted as a function of inhibitor concentration I_o [e.g., VPA, LiCl, sodium octanoate or butyrate, see Results], and the enzyme inhibition constant (K_i) was derived from the ascending part of the plot. Lineweaver-Burk plots of 1/V vs. 1/S in the presence of different inhibitor concentrations also were plotted.

Selection of the model

To determine which inhibition model best described the data, we utilized the Akaike Information Criterion (AIC) [31]

$$AIC=2k - 2\ln(L) \tag{5}$$

where k = number of parameters and L = maximized value of the likelihood function of the model. For small sample sizes, the AIC is corrected and is given by AICc [32]

$$AICc=N \times \ln(ss/N)+2K+\frac{2K(K+1)}{N-K-1} \tag{6}$$

Where ss is the sum of squares from the fit, N is the number of experimental observations and K is the number of parameters in the models. As the goodness of fit of a model to the measured data improves, the value of AIC declines. Therefore, AICc is a formal method to evaluate model quality and simplicity.

The probability that the model is correct can be determined by the following equation, where Δ is the difference between AICc scores [32]

$$\text{Probability}=\frac{e^{-5\Delta}}{1-e^{-5\Delta}} \tag{7}$$

For this current study with AA as a substrate, the lowest AICc was found for the "uncompetitive inhibition" model. The difference between AICc values for the uncompetitive and noncompetitive enzyme inhibition models was 3.266. The probability that the uncompetitive model was correct was 84%, compared to 16% for the noncompetitive model.

Using DHA as a substrate, the uncompetitive inhibition model also gave the lowest AICc. The difference between AICc was 3.178 for uncompetitive and noncompetitive enzyme inhibition. For inhibition of DHA, the probability that the uncompetitive inhibition model was correct was 83% vs. 17% for the noncompetitive model.

Data are presented as means ± S.D. Means were compared using unpaired, two-tailed Student t-tests. Linear regression analysis and other calculations were made using GraphPad Prism version 5.0 (GraphPad Software, La Jolla, CA).

Results

Enzyme expression

An optimal induction of recombinant rat Acsl isoenzyme synthesis was achieved following a 6-h incubation with 1 mM IPTG (Figure 1). The 74-kDa band of recombinant Acsl was detected by Western blotting. No signal or Acsl activity (AA as a substrate, data not shown) was observed in the *E. Coli* strain lacking a gene encoding a recombinant Acsl.

Acsl3, Acsl6v1 and Acsl6v2 kinetics

Reaction kinetics involving conversion of AA to AA-CoA by Acsl3, Acsl6v1 and Acsl6v2 in the absence of VPA followed a simple Michaelis-Menten model, as illustrated in Figure 2(a, b, c). Fitting Eq. 1 to these data gave value of K_m ranging from 23 to 48 μM for the three enzymes, and V_{max} ranging from 0.5 to 8 nmol/min/mg of protein (Table 1). Acsl3 and Acsl6v1 had similar catalytic efficiencies (maximum number of molecules of substrate that

an enzyme can convert to product per catalytic site per unit time, Eq. 2) for AA activation, $1.3 – 3 \times 10^{-5}$ min^{-1}, while the catalytic efficiency of Acsl6v2 was much less, 4×10^{-6} min^{-1} (Table 1). Also illustrated in Figure 2(a, b, c), VPA up to a concentration of 60 mM did not inhibit activation of AA to AA-CoA by Acsl3, Acsl6v1 or Acsl6v2. Triacsin C (10 μM) inhibited activation by Acsl3 by 90% (data not shown), as reported [20].

Acsl4 kinetics

With regard to Acsl4, Figure 3a illustrates that as the substrate AA concentration was elevated at different VPA concentrations in the medium, the initial velocity V for AA-CoA formation first increased, and then decreased at an AA concentration higher than about 35 μM. This biphasic pattern is consistent with substrate inhibition at high substrate concentrations (Eq. 3) [30]. In contrast, in the absence of VPA and with palmitic acid or DHA as the substrate, the reaction with Acsl4 followed simple Michaelis-Menten kinetics and the curves were asymptotic (Figures 4 and 5a).

Figure 3b presents Lineweaver-Burk plots (1/V vs. 1/[AA]) for Acsl4, at each of four VPA concentrations I_o (0, 30, 60 and 90 mM), and Figure 5b presents plots of 1/V vs. 1/[DHA] at different VPA concentrations. To calculate the plots in Figure 3b, we only considered AA concentrations in the rising phase of the V vs. [AA] curves, from 0 to 35 μM AA, since at higher AA concentrations the enzyme showed substrate inhibition (Figure 3a)., We considered the entire range of DHA concentrations because of the absence of apparent substrate inhibition in Figure 5a. The Lineweaver-Burk plots in both Figures 3b and 5b have parallel slopes at different VPA concentrations, characteristic of uncompetitive inhibition by VPA (Eq. 4) [30]. Uncompetitive inhibitors bind to the enzyme-substrate complex but not to the free enzyme, resulting in a conformational change in the enzyme. An uncompetitive inhibitor does not compete with the substrate at the same binding site, so that inhibition cannot be overcome by increasing the substrate concentration. Both K_m and V_{max} are reduced by uncompetitive inhibition.

Table 2 summarizes Michaelis-Menten parameters for Acsl4 with AA, DHA and palmitic acid as substrates, as well as catalytic efficiencies, derived by curve-fitting data in Figure 3b. In the absence of VPA, K_m for AA was 3–5 fold less than for DHA or palmitic acid. V_{max} for AA was somewhat higher than for DHA, but V_{max} for both fatty acids was about 4-fold higher than V_{max} for palmitic acid. Importantly, the catalytic efficiency of Acsl4 with AA as substrate was about 11 times higher than with DHA or palmitic acid as substrate. Acsl4 exhibited 300–2200 higher catalytic efficiency with AA as substrate than did Acsl3, Acsl6v1 or Acsl6v2 (Table 1).

VPA inhibits Acsl4-mediated acylation of AA and DHA

VPA inhibited activation by Acsl4 of AA and of DHA to their respective acyl-CoA products (Table 2 and Figures 3 and 5), but had no inhibitory effect with palmitic acid as substrate (Figure 4). Inhibition with AA and DHA as substrates is consistent with an uncompetitive mechanism (Figures 3b and 5b). The K_i for inhibition of AA and DHA acylation equaled 25 and 36 mM, respectively. Acsl4 also was 85% inhibited by 10 μM triacsin C (data not shown), as reported [20,27].

As an additional control for VPA's specificity, we tested for inhibition of AA conversion to AA-CoA by Acsl4 with sodium octanoate and butyrate. At a concentration of 60 mM, neither agent changed the kinetics of AA acylation by Acsl4 (Figure 6). To test whether Acsl4 might be a target of another mood stabilizer, we determined Acsl4 kinetics in the presence of increasing LiCl concentrations (0, 10 and 30 mM). Lithium at each concentration tested had no effect on Acsl4 kzinetics (Figure 3a).

Discussion

We characterized *in vitro* kinetics of each of four rat recombinant rat Acsl isoenzymes expressed in *E. Coli*, with regard to their conversion of AA, DHA or palmitic acid to acyl-CoA products, and examined effects of VPA and other potential inhibitors. In the absence of VPA, rat liver Acsl4 had a much lower K_m (higher affinity) for acylation of AA to AA-CoA than did rat brain Acsl3, Acsl6v1 or Acsl6v2, consistent with previous reports on rat as well as human Acsl enzymes [20,23,33]. Acsl4 had a 3 to 5-fold lower K_m with AA than with DHA or palmitic acid as its substrate, also consistent with its reported fatty acid selectivity [23]. The V_{max} of Acsl4 was about equal with either AA or DHA as substrate, but in both cases was much higher than the V_{max} with palmitic acid as substrate. The catalytic efficiency of Acsl4 was more than 10-fold higher with AA than with DHA as substrate, and 30-fold higher than with palmitate as substrate.

VPA inhibited acylation of AA and DHA by Acsl4 but not by Acsl3, Acsl6v1 or Acsl6v2. However, neither VPA's constitutional isomer, octanoate, nor its short-chain analog, butyrate, inhibited AA acylation, nor did lithium at concentrations up to 30 mM (therapeutic plasma range is 0.6–1.2 mM [1]). Thus, inhibition is specific and does not characterize all mood stabilizers.

Simple Michaelis-Menten kinetics held for AA acylation by Acsl3, Acsl6v1 and Acsl6v2, and for palmitate and DHA acylation by Acsl4 but not for AA acylation by Acsl4. The biphasic relation between velocity of AA acylation and AA concentration with Acsl4, in the absence of VPA, indicates substrate inhibition at higher AA concentrations [30]. It is unlikely that the higher AA concentrations destabilized membrane phospholipid, since increasing DHA concentrations did not reduce initial velocity.

Inhibition of AA and DHA activation by Acsl4 to their respective acyl-CoA products by VPA was characterized to be uncompetitive enzyme inhibition [30]. The K_i for VPA inhibition of AA acylation by Acsl4 was 25 mM, somewhat less than the 36 mM for DHA acylation. VPA did not inhibit palmitate acylation by Acsl4.

VPA's inhibition of AA acylation by Acsl4 is consistent with VPA's ability to reduce AA turnover in brain phospholipids of unanesthetized rats [18]. However, although VPA reduced DHA activation to DHA-CoA by recombinant Acsl4, it did not reduce DHA turnover in rat brain phospholipid [16,34]. One explanation for this discrepancy is that inhibition of acylation by Acsl4 at a given VPA concentration would have a 10-fold greater effect on AA than DHA turnover, since the enzyme's catalytic efficiency is 10-fold higher AA than for DHA acylation. The net effect would be seen, within the limits of measurement error, as a greater reduction of AA compared with DHA turnover in rat brain phospholipids.

The K_i for VPA inhibition of AA acylation by Acsl4 was 25 mM, compared with 14 mM by a rat brain microsomal preparation [16]. However, a therapeutically relevant dose of VPA (200 mg/kg, i.p.) in rats produces a brain VPA concentration of only 1.0 to 1.5 mM [17,35], about 10-fold less than either *in vitro* K_i. This difference might be reconciled if VPA within brain were at a concentration higher than the mean, consistent with evidence that it can be accumulated in mitochondria, microsomes and other organelles[36–38]. Acsl4 is present in these organelles [24,25]. The actual VPA concentration at the brain enzyme site (s) also may depend on VPA's access to Acsl4, which is localized on the inner membrane surface but, unlike the other Acsl enzymes, is not integrated within the membrane bilayer [22,26]. Furthermore, K_i for purified Acsl4 can depend on conditions such as pH in the bath medium, but the medium fatty acid or acyl-CoA binding proteins as in brain [39]. Differences between brain Acsl4 and liver Acsl4 remain to be evaluated.

It might be possible reconcile the difference between the K_i *in vitro* and the therapeutic brain VPA concentration by identifying new compounds that inhibit AA acylation by recombinant Acsl4, then testing whether these compounds also reduce AA turnover in rat brain phospholipids *in vivo* [18]. Such compounds, if identified, then could be considered for clinical trials in BD patients. A number of VPA analogs and like compounds, some of which are not teratogenic, as is VPA, because they do not inhibit histone deacetylase [40–42], could be considered in such a drug discovery paradigm.

The biologically effective concentration of an uncompetitive inhibitor may not be much less than the concentration that gives an insurmountable blockade, whereas lower concentrations may not produce much inhibition. Thus, uncompetitive inhibitors can have a relative narrow therapeutic window before toxicity intervenes [43]. This appears to be the case for VPA, whose therapeutic range in treating BD mania is between 45 to 100–125 μg/ml [44,45].

X-ray crystallography studies are unavailable for mammalian Acsl enzyme, but analysis of the crystal structure from the distantly related acyl-CoA synthetase from *Thermus thermophilus* HB8 suggests that a fatty acid-binding tunnel exists at the N-terminus [46]. Mutagenesis of Acsl4 suggests that amino acid residues at the hydrophobic end of the fatty acid binding pocket in the enzyme determine its fatty acid preference and K_m, whereas changing an amino acid at the entry of the binding pocket can inactivate the enzyme [33]. Crystallizing and then studying the mammalian enzyme could help to characterize sites of interaction with VPA and the basis of substrate inhibition by VPA.

Congenital changes in Acsl4 can lead to altered dendritic spine formation and contribute to brain disease, and a deficiency of the ACSL4 gene is associated with X-linked mental retardation [25,47]. The Alport syndrome with intellectual disability is a contiguous gene deletion syndrome involving several genes on Xq22.3 including COL4A5 and ACSL4 [48].

In summary, Michaelis-Menten analysis indicates that recombinant rat liver Acsl4 activates AA to AA-CoA by a mechanism inhibited at high substrate concentration, at a lower K_m and higher catalytic efficiency than for recombinant brain Acsl3, Acsl6v1 or Acsl6v2. Acsl4 also activates DHA to DHA-CoA without substrate inhibition. VPA uncompetitively inhibits conversion of AA to AA-CoA and of DHA to DHA-CoA by Acsl4, but not conversion of AA to AA-CoA by Acsl3, Acsl6v1 or Acsl6v2. The 10-fold greater catalytic efficiency for AA than DHA activation by Acsl4, when related to VPA's reported ability to significantly reduce AA but not DHA turnover in brain phospholipids of unanesthetized rats, suggests that inhibition of Acsl4 is the basis for the reduced AA turnover. Differences in apparent effective concentrations for the *in vitro* and *in vivo* effects might be reconciled experimentally by comparing other inhibitors of Acsl4 under the two conditions.

Acknowledgments

This work was supported by the Intramural Program of the National Institute on Aging, NIH, by NIH Grant DK 59935 (RAC), and a postdoctoral fellowship from the American Heart Association-Mid-Atlantic Region (L. O. L). We thank Professor Nina Isoherranen and Dr. Edmund Reese for their helpful comments.

Abbreviations

VPA	valproate
AA	arachidonic acid
DHA	docosahexaenoic acid
Acsl	acyl-CoA synthetase

COX	cyclooxygenase
cPLA$_2$	cytosolic phospholipase A$_2$
BD	bipolar disorder

References

1. Bowden CL. Anticonvulsants in bipolar disorders: current research and practice and future directions. Bipolar Disord 2009;11:20–33. [PubMed: 19538683]
2. Rapoport SI, Basselin M, Kim HW, Rao JS. Bipolar disorder and mechanisms of action of mood stabilizers. Brain Res Rev 2009;61:185–209. [PubMed: 19555719]
3. Kim HY, Rapoport SI, Rao JS. Altered arachidonic acid cascade enzymes in postmortem brain from bipolar disorder patients. Mol Psychiatry. 200910.1038/mp.2009.137
4. Rao JS, Harry GJ, Rapoport SI, Kim HW. Increased excitotoxicity and neuroinflammatory markers in postmortem frontal cortex from bipolar disorder patients. Mol Psychiatry 2010;15:384–392. [PubMed: 19488045]
5. Kim HW, Rapoport SI, Rao JS. Altered expressions of apoptotic factors and synaptic markers in postmortem brain from bipolar disorder patients. Neurobiol Dis 2010;37:596–603. [PubMed: 19945534]
6. Rosenberger TA, Villacreses NE, Hovda JT, Bosetti F, Weerasinghe G, Wine RN, Harry GJ, Rapoport SI. Rat brain arachidonic acid metabolism is increased by a 6-day intracerebral ventricular infusion of bacterial lipopolysaccharide. J Neurochem 2004;88:1168–1178. Erratum in: J Neurochem (2004) 1190, 1255. [PubMed: 15009672]
7. Basselin M, Kim HW, Chen M, Ma K, Rapoport SI, Murphy RC, Farias SE. Lithium modifies brain arachidonic and docosahexaenoic metabolism in rat lipopolysaccharide model of neuroinflammation. J Lipid Res 2010;51:1049–1056. [PubMed: 20040630]
8. Chang YC, Kim HW, Rapoport SI, Rao JS. Chronic NMDA administration increases neuroinflammatory markers in rat frontal cortex: cross-talk between excitotoxicity and neuroinflammation. Neurochem Res 2008;33:2318–2323. [PubMed: 18500552]
9. Clark JD, Schievella AR, Nalefski EA, Lin LL. Cytosolic phospholipase A$_2$. J Lipid Mediat Cell Signal 1995;12:83–117. [PubMed: 8777586]
10. Dennis EA. Diversity of group types, regulation, and function of phospholipase A$_2$. J Biol Chem 1994;269:13057–13060. [PubMed: 8175726]
11. Ghelardoni S, Tomita YA, Bell JM, Rapoport SI, Bosetti F. Chronic carbamazepine selectively downregulates cytosolic phospholipase A(2) expression and cyclooxygenase activity in rat brain. Biol Psychiatry 2004;56:248–254. [PubMed: 15312812]
12. Bosetti F, Rintala J, Seemann R, Rosenberger TA, Contreras MA, Rapoport SI, Chang MC. Chronic lithium downregulates cyclooxygenase-2 activity and prostaglandin E$_2$ concentration in rat brain. Mol Psychiatry 2002;7:845–850. [PubMed: 12232777]
13. Rintala J, Seemann R, Chandrasekaran K, Rosenberger TA, Chang L, Contreras MA, Rapoport SI, Chang MCJ. 85 kDa cytosolic phospholipase A$_2$ is a target for chronic lithium in rat brain. NeuroReport 1999;10:3887–3890. [PubMed: 10716228]
14. Murakami M, Kambe T, Shimbara S, Kudo I. Functional coupling between various phospholipase A2s and cyclooxygenases in immediate and delayed prostanoid biosynthetic pathways. J Biol Chem 1999;274:3103–3105. [PubMed: 9915849]
15. Bosetti F, Weerasinghe GR, Rosenberger TA, Rapoport SI. Valproic acid down-regulates the conversion of arachidonic acid to eicosanoids via cyclooxygenase-1 and -2 in rat brain. J Neurochem 2003;85:690–696. [PubMed: 12694395]
16. Bazinet RP, Weis MT, Rapoport SI, Rosenberger TA. Valproic acid selectively inhibits conversion of arachidonic acid to arachidonoyl-CoA by brain microsomal long-chain fatty acyl-CoA synthetases: relevance to bipolar disorder. Psychopharmacology (Berl) 2006;184:122–129. [PubMed: 16344985]

17. Deutsch J, Rapoport SI, Rosenberger TA. Valproyl-CoA and esterified valproic acid are not found in brains of rats treated with valproic acid, but the brain concentrations of CoA and acetyl-CoA are altered. Neurochem Res 2003;28:861–866. [PubMed: 12718439]
18. Chang MCJ, Contreras MA, Rosenberger TA, Rintala JJ, Bell JM, Rapoport SI. Chronic valproate treatment decreases the in vivo turnover of arachidonic acid in brain phospholipids: a possible common effect of mood stabilizers. J Neurochem 2001;77:796–803. [PubMed: 11331408]
19. Watkins PA, Maiguel D, Jia Z, Pevsner J. Evidence for 26 distinct acyl-coenzyme A synthetase genes in the human genome. J Lipid Res 2007;48:2736–2750. [PubMed: 17762044]
20. Van Horn CG, Caviglia JM, Li LO, Wang S, Granger DA, Coleman RA. Characterization of recombinant long-chain rat acyl-CoA synthetase isoforms 3 and 6: identification of a novel variant of isoform 6. Biochemistry 2005;44:1635–1642. [PubMed: 15683247]
21. Mashek DG, Li LO, Coleman RA. Rat long-chain acyl-CoA synthetase mRNA, protein, and activity vary in tissue distribution and in response to diet. J Lipid Res 2006;47:2004–2010. [PubMed: 16772660]
22. Li LO, Kiett EL, Coleman RA. Acyl-CoA synthesis, lipid metabolism and lipotoxicity. Biochem Biophys Acta 2010;1801:246–251. [PubMed: 19818872]
23. Soupene E, Kuypers FA. Mammalian long-chain acyl-CoA synthetases. Exp Biol Med (Maywood) 2008;233:507–521. [PubMed: 18375835]
24. Cao Y, Murphy KJ, McIntyre TM, Zimmerman GA, Prescott SM. Expression of fatty acid-CoA ligase 4 during development and in brain. FEBS Lett 2000;467:263–267. [PubMed: 10675551]
25. Meloni I, Parri V, De Filippis R, Ariani F, Artuso R, Bruttini M, Katzaki E, Longo I, Mari F, Bellan C, Dotti CG, Renieri A. The XLMR gene ACSL4 plays a role in dendritic spine architecture. Neuroscience 2009;159:657–669. [PubMed: 19166906]
26. Caviglia JM, Li LO, Wang S, DiRusso CC, Coleman RA, Lewin TM. Rat long chain acyl-CoA synthetase 5, but not 1, 2, 3, or 4, complements Escherichia coli fadD. J Biol Chem 2004;279:11163–11169. [PubMed: 14711823]
27. Kim JH, Lewin TM, Coleman RA. Expression and characterization of recombinant rat Acyl-CoA synthetases 1, 4, and 5. Selective inhibition by triacsin C and thiazolidinediones. J Biol Chem 2001;276:24667–24673. [PubMed: 11319222]
28. Bradford MM. A rapid and sensitive method for the quantitation of microgram quantities of protein utilizing the principle of protein-dye binding. Anal Biochem 1976;72:248–254. [PubMed: 942051]
29. Copeland, RA. Enzymes: A PracticalIntroduction to StructureMechanism, and DataAnalysis. 2. Wiley, John & Sons, Incorporated; New York: 2000.
30. Palmer, T. Understanding Enzymes. John Wiley; New York: 1985.
31. Akaike H. A new look at the statistical model identification. IEEE Transactions on Automatic Control 1974;19:716–723.
32. Motulsky, HaCA. Fitting models to biological data using linear and nonlinear regression: a practical guide to curve fitting. Oxford University Press; NY: 2004. p. 143-148.
33. Stinnett L, Lewin TM, Coleman RA. Mutagenesis of rat acyl-CoA synthetase 4 indicates amino acids that contribute to fatty acid binding. Biochim Biophys Acta 2007;1771:119–125. [PubMed: 17110164]
34. Bazinet RP, Rao JS, Chang L, Rapoport SI, Lee HJ. Chronic valproate does not alter the kinetics of docosahexaenoic acid within brain phospholipids of the unanesthetized rat. Psychopharmacology (Berl) 2005:1–6.
35. Loscher W, Fisher JE, Nau H, Honack D. Valproic acid in amygdala-kindled rats: alterations in anticonvulsant efficacy, adverse effects and drug and metabolite levels in various brain regions during chronic treatment. J Pharmacol Exp Ther 1989;250:1067–1078. [PubMed: 2506334]
36. Terlouw SA, Tanriseven O, Russel FG, Masereeuw R. Metabolite anion carriers mediate the uptake of the anionic drug fluorescein in renal cortical mitochondria. J Pharmacol Exp Ther 2000;292:968–973. [PubMed: 10688611]
37. Rajaonarison JF, Lacarelle B, Catalin J, Placidi M, Rahmani R. 3′-azido-3′-deoxythymidine drug interactions. Screening for inhibitors in human liver microsomes. Drug Metab Dispos 1992;20:578–584. [PubMed: 1356738]

38. Scism JL, Powers KM, Artru AA, Lewis L, Shen DD. Probenecid-inhibitable efflux transport of valproic acid in the brain parenchymal cells of rabbits: a microdialysis study. Brain Res 2000;884:77–86. [PubMed: 11082489]

39. Knudsen J, Neergaard TB, Gaigg B, Jensen MV, Hansen JK. Role of acyl-CoA binding protein in acyl-CoA metabolism and acyl-CoA-mediated cell signaling. J Nutr 2000;130:294S–298S. [PubMed: 10721891]

40. Bialer M, Yagen B. Valproic Acid: second generation. Neurotherapeutics 2007;4:130–137. [PubMed: 17199028]

41. Shimshoni JA, Dalton EC, Jenkins A, Eyal S, Ewan K, Williams RS, Pessah N, Yagen B, Harwood AJ, Bialer M. The effects of central nervous system-active valproic acid constitutional isomers, cyclopropyl analogs, and amide derivatives on neuronal growth cone behavior. Mol Pharmacol 2007;71:884–892. [PubMed: 17167030]

42. Shimshoni JA, Yagen B, Wlodarczyk B, Finnell RH, Schurig V, Bialer M. Evaluation of stereoselective anticonvulsant, teratogenic, and pharmacokinetic profile of valnoctylurea (capuride): a chiral stereoisomer of valproic acid urea derivative. Epilepsia 2010;51:323–332. [PubMed: 19674061]

43. Nahorski SR, Ragan CI, Challiss RA. Lithium and the phosphoinositide cycle: an example of uncompetitive inhibition and its pharmacological consequences. Trends Pharmacol Sci 1991;12:297–303. [PubMed: 1658998]

44. Bowden CL, Janicak PG, Orsulak P, Swann AC, Davis JM, Calabrese JR, Goodnick P, Small JG, Rush AJ, Kimmel SE, Risch SC, Morris DD. Relation of serum valproate concentration to response in mania. Am J Psychiatry 1996;153:765–770. [PubMed: 8633687]

45. Chen ST, Altshuler LL, Melnyk KA, Erhart SM, Miller E, Mintz J. Efficacy of lithium vs. valproate in the treatment of mania in the elderly: a retrospective study. J Clin Psychiatry 1999;60:181–186. [PubMed: 10192594]

46. Hisanaga Y, Ago H, Nakagawa N, Hamada K, Ida K, Yamamoto M, Hori T, Arii Y, Sugahara M, Kuramitsu S, Yokoyama S, Miyano M. Structural basis of the substrate-specific two-step catalysis of long chain fatty acyl-CoA synthetase dimer. J Biol Chem 2004;279:31717–31726. [PubMed: 15145952]

47. Bhat SS, Schmidt KR, Ladd S, Kim KC, Schwartz CE, Simensen RJ, DuPont BR, Stevenson RE, Srivastava AK. Disruption of DMD and deletion of ACSL4 causing developmental delay, hypotonia, and multiple congenital anomalies. Cytogenet Genome Res 2006;112:170–175. [PubMed: 16276108]

48. Rodriguez JD, Bhat SS, Meloni I, Ladd S, Leslie ND, Doyne EO, Renieri A, Dupont BR, Stevenson RE, Schwartz CE, Srivastava AK. Intellectual disability, midface hypoplasia, facial hypotonia, and Alport syndrome are associated with a deletion in Xq22.3. Am J Med Genet A 2010;152A:713–717. [PubMed: 20186809]

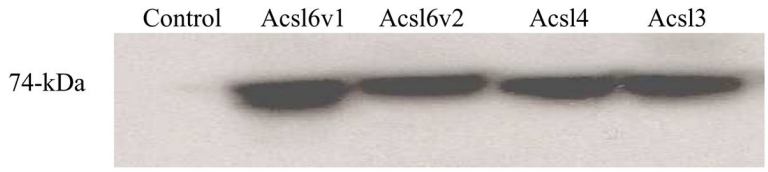

Figure 1.

Recombinant rat Acsl3, Acsl4, Acsl6v1 and Acsl6v2-Flag proteins expressed in *E. Coli* were analyzed by Western blotting with an anti-Flag M2 monoclonal antibody. Protein-antibody complexes were visualized by chemiluminescence detection of horseradish peroxidase linked to goat anti-mouse IgG. The molecular mass of the recombinant Acsl isoenzymes was 74-kDa. The same *E. Coli* strain containing the identical plasmid without the gene encoding for Acsl was used as control.

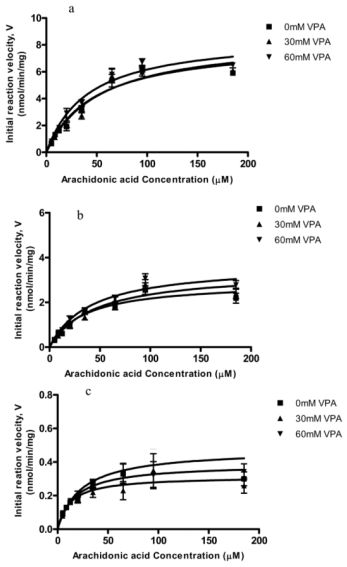

Figure 2.

Initial reaction velocity (V, nmol/min/mg protein) of (2a) Acsl3, (2b) Acsl6v1 and (2c) Acsl6v2, plotted against increasing AA concentration [S] in the presence 0, 30, or 60 mM VPA.

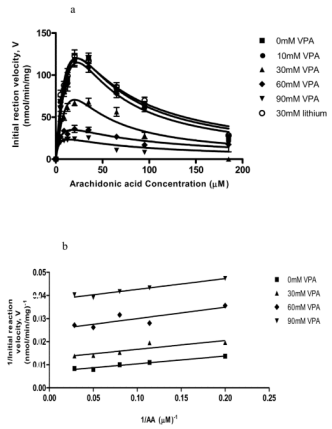

Figure 3.

(3a) Initial reaction velocity (V, nmol/min/mg protein) of Acsl4 plotted against increasing AA concentration [S] in the presence of 0, 10, 30, 60 or 90 mM VPA, or of 30 mM LiCl [I]. (3b) Lineweaver-Burk plots for the reciprocal of enzyme activity (1/V) against the inverse of substrate concentration, 1/[S] (1/[AA]).

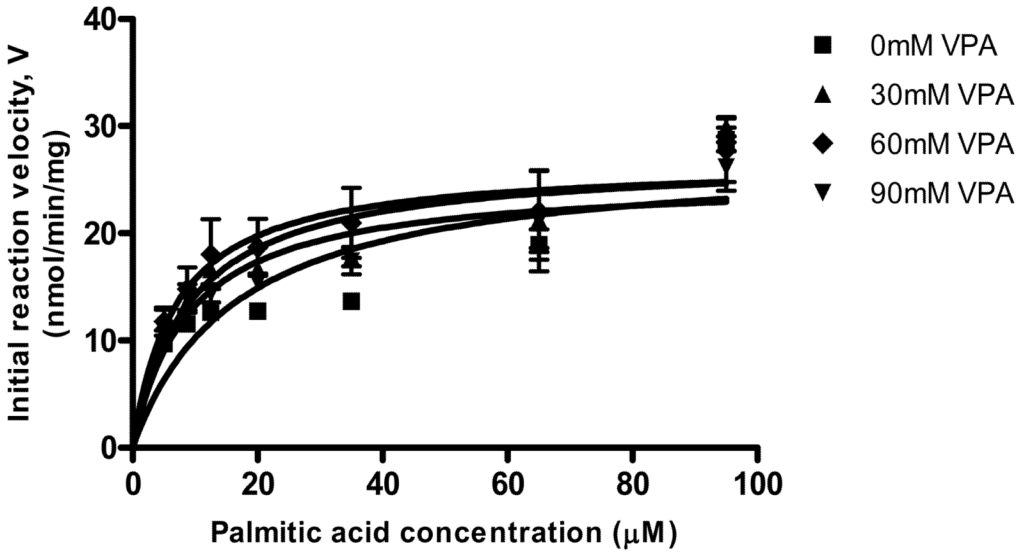

Figure 4.
Initial reaction velocity V of Acsl4 plotted against increasing palmitic acid concentration [S] in the presence of 0, 30, 60 or 90 mM VPA.

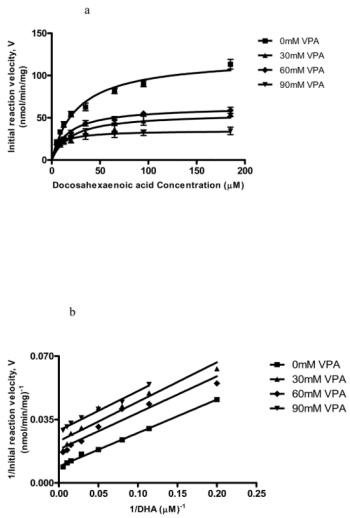

Figure 5.

(5a) Initial reaction velocity V of Acsl4 plotted against increasing DHA concentration [S] in the presence of 0, 30, 60 or 90 mM VPA. (5b) Lineweaver-Burk plots of reciprocal of enzyme activity (1/V) against 1/[S] (1/[DHA]).

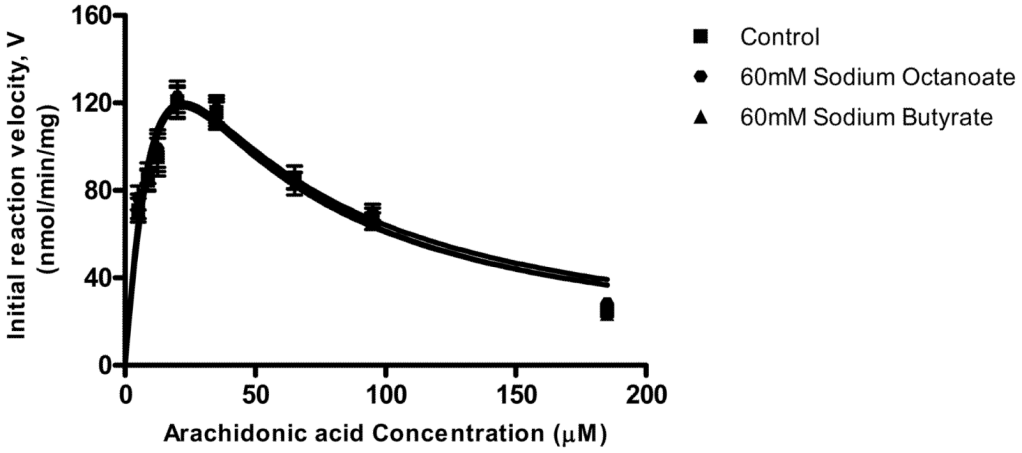

Figure 6.

Initial reaction velocity V of Acsl4 plotted against increasing AA concentration [S] in control solution, 60 mM sodium butyrate, or 60 mM sodium octanoate.

Table 1

Kinetic constants for rat recombinant Acsl3, Acsl6v1 and Acsl6v2 with AA as substrate.

Isozyme	K_m (μM)	V_{max} (nmol/min/mg)	Catalytic efficiency $V_{max}/(K_m E_T)$ (min^{-1})
Acsl3	48 ± 5	8 ± 1	$3 \cdot 10^{-5}$
Acsl6v1	34 ± 2	2.9 ± 0.5	$1.3 \cdot 10^{-5}$
Acsl6v2	23 ± 3	0.52 ± 0.08	$4 \cdot 10^{-6}$

Data are means ± SD of triplicate assays. K_m and V_{max} with AA as substrate were calculated according to the Michaelis-Menten model (Eq. 1): $V = (V_{max}S)/(K_m+S)$, where V_{max} is the maximal velocity, K_m the Michaelis-Menten constant and S the substrate concentration, determined from the data presented in Figure 2. GraphPad Prism 5 was used for best fit nonlinear regression analysis. E_T is the total enzyme concentration per reaction (mg/l).

Table 2

Kinetic constants for recombinant rat Acsl4 and K_i values for VPA

Kinetic Parameters	Substrate		
	AA	**DHA**	**Palmitic Acid**
K_m (μM)	4.98 ± 1.41	26.63 ± 3.95	16.74 ± 6.25
V_{max} (nmol/min/mg)	143.3 ± 11.1	121.4 ± 6.19	28.14 ± 3.64
K_i of VPA (mM)	24.93 ± 2.61	36.36 ± 5.22	NE
K_s of Substrate (μM)	0.86 ± 0.18	NE	NE
Catalytic efficiency $V_{max}/(K_mE_T)$ (min^{-1})	$8.79 \cdot 10^{-3}$	$7.60 \cdot 10^{-4}$	$3.19 \cdot 10^{-4}$

Data are means ± SD of triplicate assays. K_m (Michaelis-Menten constant), V_{max} (maximal initial reaction velocity) and K_S (dissociation rate constant of the substrate) of AA as substrate, were calculated by fitting the data to Eq. 3, $V = (V_{max}S)/(K_m+S(1+S/K_S)$, according to a substrate inhibition model. K_i (dissociation rate constant of VPA as an uncompetitive inhibitor) was calculated by fitting the data to Eq. 4, $V = (V_{max}S)/(K_m+S(1+S/K_S+I/K_i))$. For DHA and palmitic acid as substrates, the equation $V = (V_{max}S)/(K_m+S)$ was used to determine V_{max} and K_m, while K_i of VPA, with DHA as a substrate, was calculated by fitting the data to the equation: $V = (V_{max}S)/(K_m+S(1+I_o/K_i)$, a reduction of Eq. 3. E_T is the total enzyme concentration per reaction (mg/l). The corresponding enzyme parameters were determined from the data presented in Figures 3, 4 and 5 by using GraphPad Prism 5 for best fit nonlinear regression analysis. NE, no effect.